Proteins in Action Monitored by Time-Resolved FTIR Spectroscopy

Carsten Kötting and Klaus Gerwert*[a]

In the post genome era proteins coming into the focus of life sciences. X-ray structure analysis and NMR spectroscopy are established methods to determine the geometry of proteins. In order to determine the molecular reaction mechanism of proteins, time-resolved FTIR (trFTIR) difference spectroscopy emerges as a valuable tool. In this Minireview we describe the trFTIR difference spectroscopy and show its application on the light-driven proton pump bacteriorhodopsin (bR), the photosynthetic reaction center and the GTPase Ras, which is crucial in signal transduction. The main principles of the technique are presented, including a summary of triggering techniques, scan modes and analysis.

Introduction

Time-resolved Fourier-transform infrared (trFTIR) difference spectroscopy can reveal great molecular detail of the reaction mechanisms of proteins.[1,2] This manuscript mainly describes the basic idea of the approach and uses the work of our lab as examples; it is not a detailed review of all the FTIR literature. For further literature the reviews of Heberle,[3] Mäntele,[4] Vogel and Siebert,[5] Rothschild,[6] Braiman and Rothschild,[7] Maeda,[8] Barth,[9] Kandori[10] and Breton[11] are suggested.

By the performance of difference spectra, one can select the absorbance bands of the protein groups that are involved in the reaction out of the background absorbance of the whole sample. The absorbance changes can be monitored with time resolutions down to nanoseconds and followed for time periods ranging over nine orders of magnitude. This technique is suitable for many proteins, including membrane proteins with sizes up to 100 000 Daltons.[12]

This technique can provide information that is complementary to X-ray structure analysis, including information on:

- the H-bonding,
- the protonation state,
- the charge distribution,
- the time dependence of the protein reactions.

TrFTIR of proteins was introduced in the study of the light-driven proton pump bacteriorhodopsin (bR).[13] The first fast-scan studies provided the key protonation steps: the deprotonation of the central proton binding site, the protonated Schiff base, and the protonation of the counterion Asp85 and reprotonation by protonated Asp96. Furthermore, the coupling of the light-induced electron transfer to the proton uptake, a key step in photosynthetic proteins, was elucidated based on step-scan FTIR measurements.[12] Further, the catalysis of the GTPase reaction of Ras proteins by a protein–protein interaction with GAP (GTPase activating protein) proteins was monitored in real time using caged GTP as a photolabile trigger.[14]

Difference Spectroscopy

Even a relatively small protein of 20 kD has about 10^4 vibrational modes. Thus, from the absorption spectrum alone (Figure 1 A) one cannot obtain information on individual bands but only on the global features of the protein. The spectrum is dominated by the amide I (C=O stretch) and amide II (NH bend coupled with C–N stretch) bands, to which every amino acid contributes. From these backbone absorptions information on the secondary structure can be gained. In an analysis of the amide I band, its components (α-helix, β-sheet and turn) can be fitted by separated curves, because different hydrogen bonding leads to shifts of the band.[15] Water absorptions (O–H bend) are found in the same region as the amide I; thus, this analysis is easier to perform in samples dissolved in D_2O, which absorbs around 1250 cm^{-1}.

For an FTIR difference spectrum (Figure 1 B) of a reaction A→B, one calculates the absorbance spectrum of B minus the absorbance spectrum of A. Thus, the vibrations from groups that are not changed during the reaction annihilate each other, and only the changes during the reaction are seen. Individual absorptions can then be resolved. It is important to maintain accurately the same conditions during the reactions, otherwise the background, with a 10^3 stronger absorbance (see Figure 1 A), will obscure the difference spectrum. To demonstrate the signal-to-background ratio, the difference spectrum is also shown on the bottom of Figure 1 A at the same scale. To monitor such small changes, of the order of 10^{-3} to 10^{-4} absorbance units, highly sensitive instrumentation is required. FTIR spectroscopy is able to detect such small changes reliably.

[a] *Dr. C. Kötting, Prof. Dr. K. Gerwert*
Lehrstuhl für Biophysik, ND 04/596, Ruhr-Universität Bochum
44801 Bochum (Germany)
Fax: (+49) 234-14238
E-mail: koetting@bph.rub.de
gerwert@bph.rub.de

 DOI: 10.1002/cphc.200400504

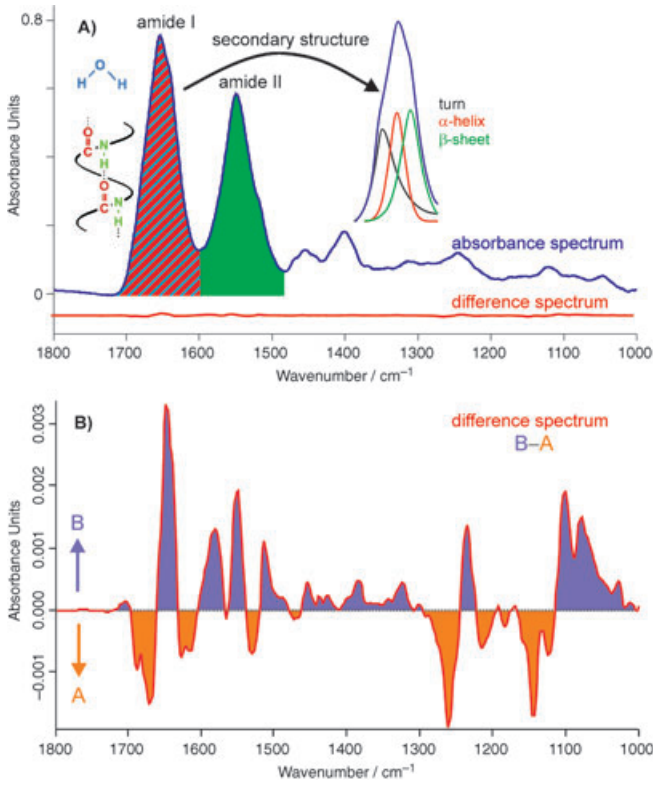

Figure 1. *A) Typical IR absorbance spectrum of a protein (Ras). The main components are indicated by the colors red (amide I), blue (water) and green (amide II). In a secondary structure analysis, the components (α-helix, β-sheet and turn/coil) of the amide I band can be separated. To the bottom, an IR difference spectrum of the same protein for the hydrolysis reaction (Ras·GTP→Ras·GDP) is shown. B) The same difference spectrum as in (A), with enlarged scaling. Individual absorptions of phosphate and protein bands, which change during the reaction, are resolved.*

Experimental Section

A typical setup for a time-resolved FTIR experiment consists of a light source, an interferometer, sample chamber, and a detector. The sample chamber is equipped, for example, with a thermostatic transmission cell in which the sample is placed. For triggering, the sample in the cell can also be irradiated by a laser. Finally, the infrared light reaches, for example, a liquid-nitrogen-cooled MCT (mercury–cadmium–telluride) detector.

The most common cell is a simple transmission cell with IR-transparent windows (e.g. CaF_2). To reduce the water background absorption, fully hydrated films, which are a few μm thick, are used. As an alternative to transmission cells, ATR (attenuated total reflection) cells can be used.[16–18] In this setup, the IR light is reflected at the interface of a crystal (most commonly diamond, ZnSe, or Ge) and the sample. Since, in this process, an evanescent wave penetrates only a few μm into the sample, the protein film can be much thicker than in the transmittance cell. The lower the distance of the absorbing species to the crystal, the stronger the absorption. This effect can be enhanced by the SEIRA (surface-enhanced infrared absorption reflectance) technique, where the ATR cell is coated by a thin film of gold or silver.[19–21] In this way, thin layers (e.g. of lipids) can be investigated. One can increase the absorption further by using multiple reflections. ATR cells with 1 to 25 reflections are available.

Both, transmission cells and ATR cells can be used as flow cells. In either case, the sample can be easily exchanged by means of a tubing system. This can increase the quality of difference spectra enormously, because the whole setup (sample thickness, window position etc.) can be maintained exactly the same. This is not possible if the sample has to be removed from the spectrometer and the transmittance cell has to be reassembled with the new sample. Further, use of an ATR flow cell creates possibilities for the investigation of protein–protein interactions:[22] for example, one protein can be immobilized in a lipid layer, fixed to an ATR crystal,[23] or bound via an anchor at the ATR surface.[24] The interaction of the attached protein with other proteins in the liquid phase can then be studied.

Trigger Techniques

The difference technique requires a sharp initiation (triggering) of the protein reaction. This can be achieved by a laser flash that activates a protein (A), by release of a caged compound (B), or by fast mixing (C), as described below:

A) Photobiological systems: Light-induced reactions in photobiological systems, such as bacteriorhodopsin (bR)[25,26] or photosynthetic reaction centers (RCs),[12] which carry intrinsic chromophores (e.g. Retinal, Figure 2 A), are ideally suited to time-resolved studies. In these systems, the chromophore can be directly activated by a laser flash, enabling isomerization or redox reactions of prosthetic groups and subsequent reactions.

B) Caged compounds: A broad range of applications can be achieved using caged compounds in which biologically active molecules are released from inactive photolabile precursors. They allow the initiation of a protein reaction with a nanosecond UV laser flash. Caged phosphate, caged GTP, caged ATP, and caged calcium have been established as particularly suitable trigger compounds.[27,28] The most popular caging groups are *ortho*-alkylated nitrophenyl compounds.[29] However, photoreactions of such compounds involve several intermediates, which limits the time resolution for the reaction. The *para*-hydroxyphenacyl cage (pHP-), where the reaction proceeds on the excited state in the sub-nanosecond time regime without intermediates, is faster.[30] In Figure 2 B, the photochemical activation of pHP-GTP is shown. The photolysis reaction of caged GTP has been investigated in detail by FTIR spectroscopy. Bands were assigned by the use of ^{18}O phosphate labeling by Cepus et al.[31] In addition, FT-Raman spectra and photolysis spectra of caged Ca^{2+} have been reported.[31]

C) Mixing Cells: Another approach for starting reactions is fast mixing of the reaction partners. This can be achieved in a stopped flow setup where the two components are mixed and transferred into the sample chamber.[32] Even faster mixing is possible using continuous flow systems. We have developed a micro mixing cell (Figure 2 C), which allows mixing of two components within the sub-millisecond time regime.[33] Since silicon is transparent in the mid-infrared, micromachined silicon components offer great potential for establishing FTIR spectroscopy as a method for studying microsecond mixing experiments. The protein solution is in the center and two streams of another solution (e.g. another protein, ligand, or

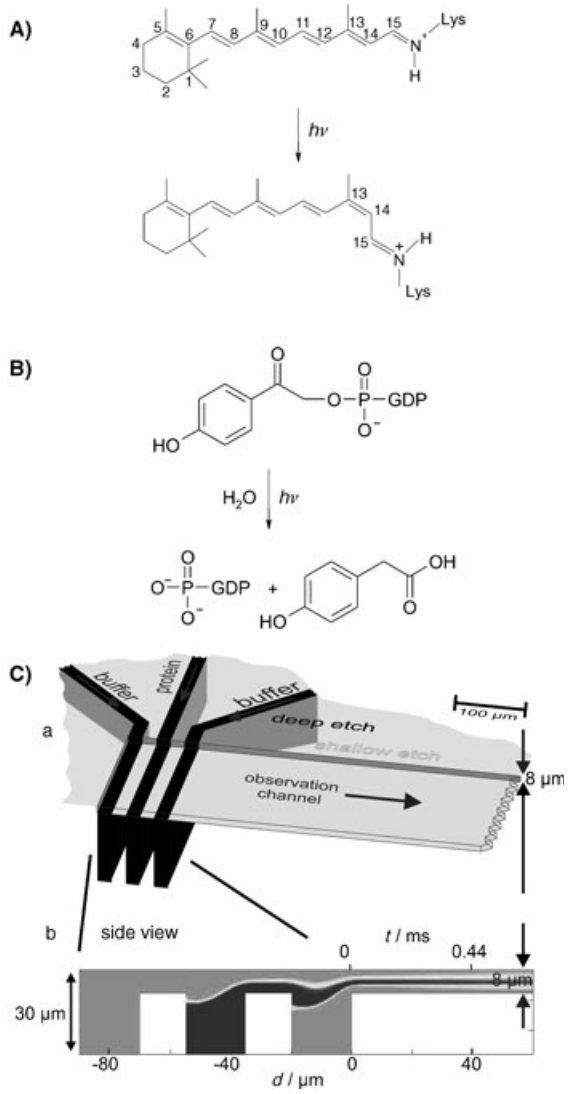

Figure 2. *Different options for triggering a reaction: A) Photobiological systems can be triggered directly by a laser flash. B) Caged compounds set free the desired compound after a laser flash. The pHP-caged GTP sets free GTP within 500 ps. C) Triggering by mixing is, for example, possible in a microfabricated flow cell. In the side view (b), a fluid dynamics simulation for the mixing of a protein solution (black) with a buffer (grey) by diffusion is shown. Note that the observation channel is much longer than the part shown here. More details are given in ref. [33].*

buffer) enter through 30-μm-deep inlet channels, which intersect with the 8-μm-deep observation channel. Due to the viscosity-determined laminar flow, no turbulence is induced when the buffer channels merge, and a layer of the center solution between two outer layers over the whole width of the observation channel results. Since the layers are thin, diffusing reactant molecules stream from one solution into the other, and thus, mixing is fast. The time resolution is achieved by scanning along the observation channel with the focused beam of an FTIR microscope. The time resolution is a function of the diffusion coefficient and thus dependent on the size of the proteins. For small molecules, a time resolution of 400 μs can be achieved. This is about 300 times faster than current IR stopped-flow setups. Additionally, the miniaturization used to create such cells reduces sample consumption.

Rapid Scan

The principle of the rapid-scan FTIR mode of time-resolved spectroscopy is simple: after taking a reference spectrum of the protein in its ground state, one activates the protein (e.g. by a laser flash) and records interferograms in shorter times than the half-lifes of the reactions.[26] The time resolution of this method depends on the sampling time for an interferogram and is about 10 ms. In a kinetic analysis (see below) amplitude spectra for the individual conversions can be calculated.

Step Scan

In the step-scan mode, the interferometer moving mirror may be visualized as being held stationary at the interferogram mirror position x_n. The protein activity is initiated, for example, by a laser flash, and the time dependence of the intensity change at this interferogram position x_n is measured. Then the interferometer "steps" to the next interferogram data position x_{n+1}, and the reaction is repeated and measured again. This process is continued at each sampling position of the interferogram. The time resolution is usually determined by the response time of the detector, which is about a few nanoseconds. After the measurement, the data are rearranged to yield time-dependent interferograms $I(t_i)$. Extended discussions of the step-scan technique can be found in refs. [34–38].

Kinetic Analysis

For the analysis of time-resolved data, it is important to analyze the kinetics of the observed reaction. A global-fit analysis yields the apparent rate constants of the analyzed processes.[39] The global-fit analysis not only fits the absorbance change at a specific wavenumber, but at up to 800 wavenumbers in the spectrum simultaneously. All reactions are assumed to be first order and can therefore be described by a sum of n_r exponentials. The fit procedure minimizes the difference between the measured data $\Delta A_{measured}$ and the theoretical description ΔA, shown in Equation (1), weighted according to the noise at the respective wavenumbers, and summarized not only over the time but also over the wavenumbers.

$$\Delta A(\nu,t) = \sum_{l=1}^{n_r} a_l(\nu) e^{-k_l t} + a_0(\nu) \qquad (1)$$

An alternative method of data analysis is the singular value decomposition or principal component analysis (PCA) approach,[39] in which a set of basis difference spectra are calculated from all the measured difference spectra. This procedure allows the determination of transient spectra independently from specific kinetic models or temporal overlap.[39,40] Thus, this approach should be used if the reactions are not first-order.

Band Assignments

A large number of spectral bands can be seen in the difference spectrum in Figure 1B. The frequency range in which a band appears allows a tentative assignment of the bands; for example, carbonyl vibrations of aspartic or glutamic acids absorb between 1700 and 1770 cm^{-1}. In order to draw detailed conclusions from the spectra, the bands have to be assigned to individual groups. Unambiguous band assignment can be performed by using isotopically labeled proteins[41] or by amino acid exchange via site-directed mutagenesis.[26]

The principle of band assignment by site-directed mutagenesis is demonstrated in Figure 3A in the example of the bR–N difference spectra of the wild type (WT) and the Asp–96–Asn mutant.[26] Absorbance changes in the spectral range between 1500 and 1000 cm^{-1} (not shown) are highly reproducible, which indicates that this specific mutagenesis is noninvasive and does not disturb the protein structure. Only the carbonyl band shift at 1742 cm^{-1} is absent in the spectrum of the mutant. This is the 4-carbonyl vibration of the exchanged Asp96,[26] which demonstrates that this group deprotonates in the N intermediate.

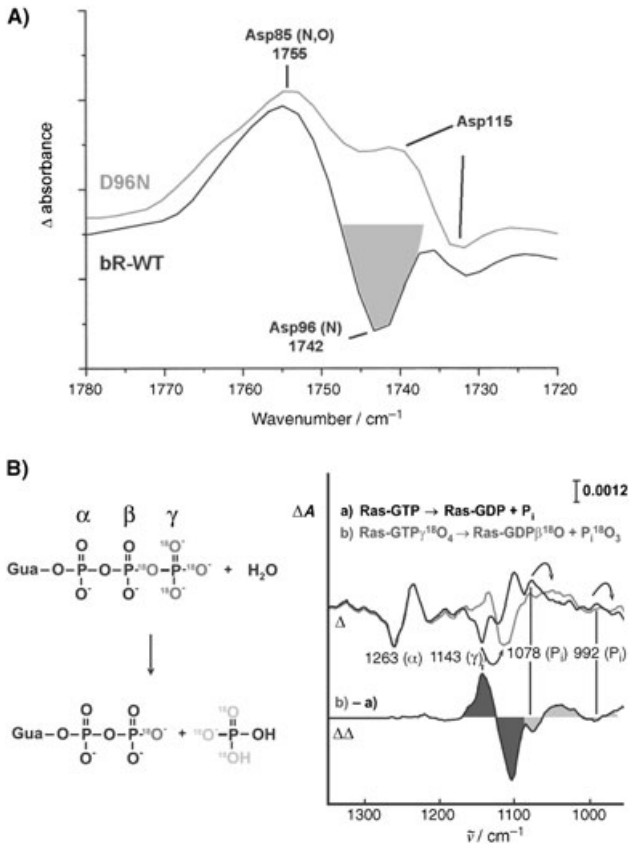

Figure 3. *A) Spectra demonstrating the principle of band assignment by site-directed mutagenesis. Difference spectra (N-bR) of bR are shown. The spectrum of the bR-wt shows a negative band of Asp96. In the corresponding spectrum of the mutant Asp 96 Asn, this band is absent. Additionally, the difference bands of Asp115 are now seen more clearly. B) Spectra demonstrating the principle of band assignment by isotopic labeling. In black the hydrolysis spectrum of Ras·GTP to Ras·GDP is shown, in grey the same with $\gamma^{18}O$-labeled GTP. The band at 1143 cm^{-1} is shifted and can be assigned to a γ-vibration, whereas the band at 1263 cm^{-1} (the α-band) is not affected.*

Mutation of an amino acid changes the structure of the protein to a greater or lesser degree, and it is easy to achieve by site-directed mutagenesis, a standard molecular biology method.[42] On the other hand, isotopic labeling has the advantage of marking the molecular group noninvasively:

Isotopic labeling shifts the stretching frequency of the labeled group due to the increased reduced mass, μ. The frequency, ν, is given by:

$$\nu = \frac{1}{2\pi}\sqrt{\frac{k}{\mu}} \qquad (2)$$

where k is the force constant. Isotopic labeling can be performed on prosthetic groups, such as retinal,[43] or nucleotides, such as GTP.[14,31,44] These compounds can be chemically synthesized. Isotopic labeling of all amino acids of one kind can be achieved by biosynthetic incorporation of isotopically labeled amino acids, for example, aspartic acid.[41] As an example, site-specific isotopically labeled caged GTP is presented in Figure 3B. Here $\gamma^{18}O_4$-labeled GTP is used in the Ras-catalyzed hydrolysis reaction of GTP.[44] In the difference spectrum (Δ) of the hydrolysis the negative bands correspond to the Ras·GTP state. The band at 1143 cm^{-1} is shifted by the γ label and can thus be assigned to an absorption of the γ-GTP group. On the other hand, the α band at 1263 cm^{-1} (assigned by α-labeled GTP, not shown) remains in the same position after γ labeling. Similarly, one can assign positive bands (product state) at 1078 and 992 cm^{-1} as absorptions of the appearing P_i after hydrolysis. Often, a double-difference spectrum ($\Delta\Delta$), the difference of the labeled and the unlabeled difference spectra, gives distinct band positions, because only absorptions that shift due to the labeling appear.

The most powerful method for band assignment is site-directed isotopic labeling of an amino acid. This is an expensive molecular biology method and only very rarely successfully applied. However, it is clear that chemical synthesis of a protein can allow site-directed isotopic labeling and may become the method of the future.[45,46] Once a band is assigned, very accurate information on interactions of this group, protonation states, charge distribution, involvements in the reaction mechanisms, and bond orders can be obtained.

QM/MM Calculations or Theoretical FTIR Spectroscopy of Proteins

With the QM/MM (quantum mechanics/molecular mechanics) approach,[47] IR spectra of proteins can be calculated. Because proteins are far too large to be treated completely quantum chemically, the major part of the protein and its water surrounding are classically calculated using an empirical force field at a lower computational level, but the active center or a prosthetic group bound to the protein is treated by high-level quantum mechanical methods, mostly density functional theory (DFT). Thereby, the dynamics of the protein surroundings are regarded in contrast to vacuum ab initio calculations.

The QM/MM calculations provide the frequency, the bandwidth, and the intensity of infrared absorptions. By comparison with experimentally observed spectra, the accuracy of the calculation can be evaluated. If the vibrational spectrum is well reproduced, the results obtained from the calculation will be reliable. The QM/MM calculations provide the geometry, the electron density, and the charge distribution of the QM-treated protein part. These are the crucial parameters, which determine the molecular mechanism of a protein. By using this approach, first phosphate in water[48] and then GTP bound to Ras[49] have been calculated. The theoretical spectra agree reasonably with the experimentally observed ones. The experimentally observed downshift of the β-phosphate vibration comparing GTP in water and GTP bound to Ras can be quantitatively correlated to a charge shift towards β-phosphate from γ- and α-phosphate due to protein binding. This charge shift was predicted to reduce the free activation energy, and it thereby catalyses the reaction. These results show that this is a promising approach to decode more quantitative information from IR spectra.

Examples of FTIR Spectroscopic Investigations of Protein Action

How Proteins Pump Protons

After light excitation of bacteriorhodopsin's (bR) light-adapted ground state, BR_{570}, a photocycle starts with the intermediates J_{610}, K_{590}, L_{550}, M_{410}, N_{530}, and O_{640}, distinguished by the different absorption maxima given by the indices. During the rise of the M-intermediate a proton is released to the extracellular side, and during the M-decay a proton is taken up from the cytoplasmic side. This creates a chemic–osmotic proton gradient across the membrane.

The absorbance changes accompanying this reaction pathway can be monitored by the step-scan FTIR technique with a time resolution of 30 ns.[38] In Figure 3, the IR absorbance changes between 1800 and 1000 cm^{-1} during the photocycle are shown in a three-dimensional representation. Beyond a background absorbance of up to one absorbance unit, changes on the order of 10^{-3} to 10^{-4} are monitored with 3-cm^{-1} spectral resolution and 30-ns time resolution.

The appearance of the C–C stretching vibration band at 1190 cm^{-1} indicates the all-*trans* to 13-*cis* isomerization of retinal. It takes place within 450 fs and is not time-resolved here. Its disappearance at about 200 μs indicates the deprotonation of the Schiff base. This loss of charge of the Schiff base greatly reduces the IR absorbance of the chromophore. (The Schiff base connects the retinal to Lys216 of the protein, see Figure 4B). The deprotonation kinetics of the Schiff base agrees nicely with the protonation kinetics of the counterion Asp85, which can be followed at 1761 cm^{-1} (Figure 4B).[26] Recently, for the proton-release pathway to the protein surface, a protonated hydrogen-bonded network has been identified (Figure 4).[50] According to a combination of X-ray data,[51] FTIR measurements,[52] pK_a calculations,[53] and molecular dynamics calculations,[54] the $H_5O_2^+$ complex is believed to be stabilized between Glu204 and Glu194. This complex can be identified in the FTIR spectrum by a continuum band between 1800 and 1900 cm^{-1}. The reprotonation of the Schiff base by Asp96 is indicated by the reappearance of the band at 1190 cm^{-1} in the millisecond time domain.[26,55] The final disappearance at 1190 cm^{-1} shows the chromophore's relaxation to the all-*trans* BR ground-state configuration. Based on the FTIR experiments, a detailed model of the light-driven proton pump bacteriorhodopsin has been elucidated and is presented in Figure 4B.

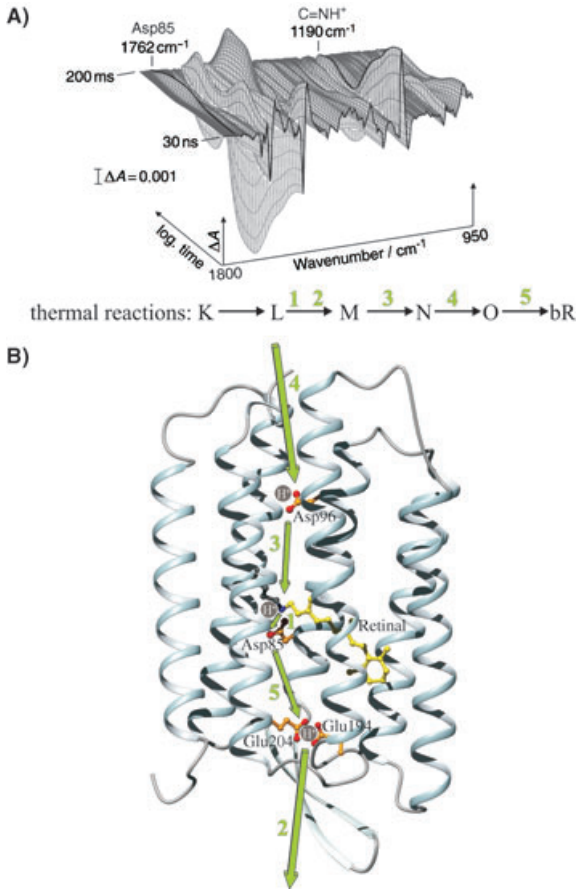

Figure 4. *A) The IR absorbance changes during the photocycle of bR. One band of the protein at 1762 cm^{-1} (protonated Asp85) and one of the protein–ligand interface at 1190 cm^{-1} (protonated Schiff base) are marked. B) Model of the proton–pump mechanism of bR, to which many groups have contributed (for references, see text). After the light-induced all-*trans* to 13-*cis* retinal isomerization in the BR-to-K transition, the Schiff base proton is transferred to Asp85 in the L-to-M transition (**1**). Deprotonation of the protonated Schiff base can be followed at 1190 cm^{-1} in (a) and protonation of Asp85 at 1762 cm^{-1} in (a). Simultaneously (**2**), an excess proton is released from an Zundel-like[67] hydrogen-bonded network of internal water molecules to the extracellular site. Glu204, Glu194, and Arg82 control this network. Asp85 reprotonates the network in the O-to-BR reaction (**5**). The Schiff base is oriented in the M1-to-M2 transition from the proton-release site to the proton-uptake site, and thereby determines the direction of the proton transfer. A larger backbone movement of the helix F is observed in the M-to-N transition compared with the M1-to-M2 transition. Asp96 reprotonates the Schiff base in the M-to-N transition via waters in a Grotthuss mechanism (**3**), also seen at 1190 cm^{-1} in (a). Deprotonation of Asp96 can also be seen at 1742 cm^{-1} in Figure 3B. Asp96 itself is reprotonated from the cytoplasmic site in the N-to-O transition (**4**).*

How Light-Induced Electron Transfer Is Coupled to Proton Uptake in Photosynthesis

Photosynthesis transforms light energy into chemical energy. The photons oxidize a primary donor, typically a chlorophyll embedded within a photosynthetic protein. The released electron is then transferred within the same complex via prosthetic groups to a final electron acceptor, typically a quinone. The reduced quinone is protonated from the bulk and than released by the photosynthetic protein. This creates a proton gradient across the membrane, which drives ATP synthesis.

The light-induced changes in the 100 kD photosynthetic reaction center (RC) of *Rhodobacter sphaeroides* were monitored from 30 ns to 35 s by FTIR difference spectroscopy (Figure 5 A).[12] The bacterial photosynthetic reaction center is structurally very similar to D_1/D_2 subunits of photosystem II.[56,57] The results provide detailed mechanistic insights into the coupling of the light-induced electron transfer to the proton uptake in the Q_A-to-Q_B transition. This is a crucial step in the energy transduction. Based on absorbance changes observed in photolysis experiments in the visible spectral range it was earlier concluded that the fast absorbance changes represent electron-transfer reactions and the slower proton uptake.[58] However, the visible absorbance changes cannot clearly distinguish between electron- and proton-transfer reactions, mainly redox changes of prosthetic groups are monitored. From X-ray structure analysis it was concluded that a so-called propeller-twist movement of Q_B represents a conformational gating for the Q_A to Q_B transition, because different positions of Q_B are observed in dark and light-adapted samples.[59] In contrast, time-resolved FTIR experiments show different Q_B positions already in the dark-adapted samples and show that the propeller-twist movement does not take place in the Q_A-to-Q_B transition. In contrast to the earlier proposals in the literature, based on the results of the FTIR experiments, a new molecular mechanism is proposed (see Figure 5): reduction of Q_A in picoseconds (**1**), which induces protonation of histidines (**2**), probably of His126 and His128 in the H subunit at the entrance of the proton-uptake channel, and of Asp210 in the L subunit inside the channel at 12 and 150 μs. This and not the propeller-twist movement, as suggest earlier by the X-ray analysis, seems to be a prerequisite for the reduction of Q_B (**3**), Q_A^- is reoxidized at 1.1 ms, and a proton is transferred from Asp210 to Glu212 (**4**). Glu212 is the proton donor to Q_B^-. The data indicate that Q_B is not reduced directly by Q_A^- but presumably through an intermediary electron donor. This intermediate was resolved for the first time by trFTIR spectroscopy. The His190(L)–Fe^{2+}–His219(M) moiety is optimally positioned between Q_A and Q_B to donate the electron to Q_B. Mutations of His219(M) or exchange of the Fe^{2+} substantially alters the electron transfer from Q_A^- to Q_B. However, it is not yet clear, if the non-heme Fe undergoes a redox reaction itself, or other groups are involved, for example His190. Further experiments are required to clarify this question. Up to now a redox reaction of Fe was excluded in bacterial reaction centers, but not in the structurally homolog photosystem II. However, the intermediary electron donor seems to have an unusual shift in its redox potential.

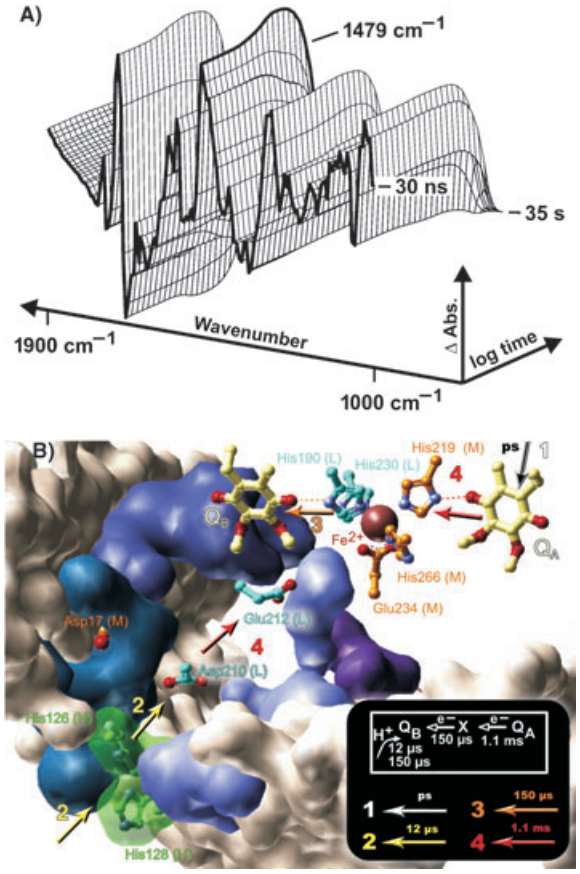

Figure 5. *A) Representation of the light-induced IR absorbance changes in the photosynthetic reaction center of Rb. Sphaeroides with 30-ns time resolution and 7-cm^{-1} spectral resolution as revealed by global-fit analysis according to the given formula. The time axis has a logarithmic scale to show the complete reaction over nine orders of magnitude (30 ns to 35 s) in one representation. B) Light-induced electron transfer from P to Q_A takes place within 200 ps via overlapping prosthetic groups (**1**). Based on the results of the FTIR experiments a new molecular mechanism is proposed for the following steps: protonation of histidines (**2**), probably of His126 and His128 in the H subunit at the entrance of the proton-uptake channel, and of Asp210 in the L subunit inside the channel at 12 and 150 μs. This seems to be a prerequisite for the reduction of Q_B (**3**). Q_A^- is reoxidized at 1.1 ms, and a proton is transferred from Asp210 to Glu212 (**4**). Glu212 is the proton donor to Q_B^-. The data indicate that Q_B is not reduced directly by Q_A^- but presumably through an intermediary electron donor. This intermediate has been resolved for the first time by trFTIR spectroscopy.*

How Ras GTPases Work

GTPases, which catalyze the hydrolysis of GTP to GDP and P_i, play a key role in the regulation of many biological processes.[60] Ras is the prototype of the family of GNBPs, which contain a structurally highly conserved G domain. In oncogenic Ras the activation of Ras GTPase activity is inhibited, and this is thought to be the central event in Ras-dependent transformation of a cell into a cancer cell.

The time course of the GTPase reaction of Ras and the protein–protein complex Ras·RasGAP was measured by FTIR spectroscopy. The reaction is started by a laser flash using pho-

tolabile caged GTP bound to Ras. The laser flash releases Ras·GTP, which subsequently undergoes a Ras-mediated GTPase reaction. Binding of GTP to Ras already induces a more productlike (GDP) charge distribution in the educt (GTP) state and thereby reduces the free activation energy for hydrolysis. This involves a shift of negative charge towards the β-phosphate of GTP, indicated by a red-shift of the corresponding absorption.[44,61,62] This seems the main contribution to catalysis. The charge distribution in GTP cannot be resolved in the X-ray structural analysis, but with IR data in combination with QM/MM (quantum mechanic/molecular mechanic) calculations. Therefore, the FTIR is a good complementary technique to the powerful X-ray analysis and provides detailed information on the reaction mechanism beyond the structure.

The GTPase reaction is further regulated by a GTPase-activating protein (GAP). Detailed analysis of the GTPase reaction of the protein complex of Ras and RasGAP[14] shows three key differences:[14]

- The reaction with the protein–protein complex is accelerated by a factor of 10^5.
- The Ras·GAP reaction involves an intermediate. In this intermediate, the γ-phosphate is already cleaved from the remaining GDP, but remains within the binding pocket.
- The β-band of GTP, which is—compared to GTP in water—downshifted in Ras, is even further downshifted in Ras·GAP. This indicates an additional substantial shift of negative charge towards the β-phosphate. The charge shift is provided by the Arg finger of the GAP, which pulls negative charge towards the β-phosphate, as do the Mg and Lys of Ras (Figure 6). The shift towards the β- but not the γ-phosphate was not expected according to transition-state models,[63] but was recently affirmed by theoretical methods[49] and measurements of kinetic isotope effects.[64]

Due to the additional kinetic information in time-resolved FTIR difference spectroscopy information on thermodynamic parameters can be gained by means of Arrhenius plots and application of transition-state or Kramers' theory.[62] By performing kinetic measurements at different temperatures, the entropy and enthalpy contributions to the activation barrier of the hydrolysis reaction were estimated. The entropic contributions to the catalytic effect are only minor in GTPase catalysis and the enthalpic contributions from electrostatic interactions (the charge shift towards β-phosphate) are key to the catalysis.

Acknowlegments

Financial support of SFB 480 and SFB 642 of the DFG is gratefully acknowleged.

Keywords: IR spectroscopy · isotopic labeling · proteins · reaction center · time-resolved spectroscopy

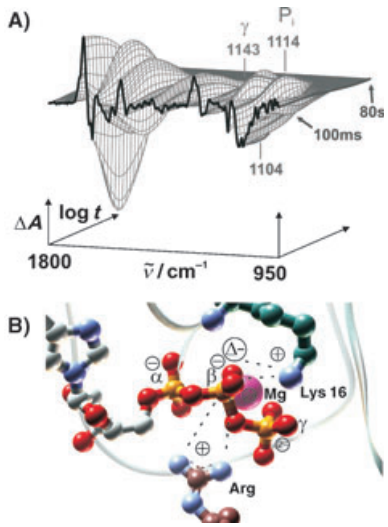

Figure 6. *A) Time-resolved infrared absorbance difference spectra during the GAP-catalyzed GTPase reaction of Ras. The global fit is a sum of three exponential functions, giving rise to two intermediates, as seen at 1143 and 1114 cm^{-1}, respectively. At 1143 cm^{-1} the appearance of GTP from caged GTP and GTP hydrolysis is observed. At 1114 cm^{-1} the protein bound P_i appears, and is released in the rate-limiting step to the external bulk medium. Compared with the intrinsic reaction, it is catalyzed by several orders of magnitude. To the right, the structural models of GAP·Ras bound to GTP is shown.[65] B) Schematic representation showing the influence of the Ras·GAP protein–protein complex on GTP, which leads to the catalytic effect. The global picture is obtained by X-ray structural models of a transition state analog,[66] the details are resolved by FTIR spectroscopy:[14] P-loop, Mg, and Lys of Ras shift negative charge toward the β-phosphate. This effect is enhanced by the arginine finger of the GAP.*

[1] K. Gerwert, *Ber. Bunsen-Ges.* **1988**, *92*, 978.
[2] K. Gerwert, *Curr. Biol. Curr. Opin. in Struct. Biol.* **1993**, *3*, 769.
[3] J. Heberle, *Biochim. Biophys. Acta* **2000**, *1458*, 135.
[4] W. Mäntele, *Trends Biochem. Sci.* **1993**, *18*, 197.
[5] R. Vogel, F. Siebert, *Curr. Opin. Chem. Biol.* **2000**, *4*, 518.
[6] K. J. Rothschild, *J. Bioenerg. Biomembr.* **1992**, *24*, 147.
[7] M. S. Braiman, K. J. Rothschild, *Annu. Rev. Biophys. Biophys. Chem.* **1988**, *17*, 541.
[8] A. Maeda, *Isr. J. Chem.* **1995**, *35*, 387.
[9] A. Barth, C. Zscherp, *Q. Rev. Biophys.* **2002**, *35*, 369.
[10] H. Kandori, *Recent Res. Dev. Phys. Chem.* **2001**, *5*, 161.
[11] J. Breton, *Biochim. Biophys. Acta* **2000**, *1507*, 180.
[12] A. Remy, K. Gerwert, *Nat. Struct. Biol.* **2003**, *10*, 637.
[13] K. Gerwert, G. Souvignier, B. Hess, *Proc. Natl. Acad. Sci. USA* **1990**, *87*, 9774.
[14] C. Allin, M. R. Ahmadian, A. Wittinghofer, K. Gerwert, *Proc. Natl. Acad. Sci. USA* **2001**, *98*, 7754.
[15] K. A. Oberg, J.-M. Ruysschaert, E. Goormaghtigh, *Protein Sci.* **2003**, *12*, 2015.
[16] N. J. Harrick, *Applied Spectroscopy* **1987**, *41*, 1.
[17] U. P. Fringeli, D. Baurecht, M. Siam, G. Reiter, M. Schwarzott, T. Burgi, P. Bruesch, *Handbook of Thin Film Materials* **2002**, *2*, 191.
[18] S. A. Tatulian, *Biochemistry* **2003**, *42*, 11 898.
[19] M. Osawa, *Topics in Applied Physics* **2001**, *81*, 163.
[20] K. Ataka, J. Heberle, *J. Am. Chem. Soc.* **2003**, *125*, 4986.
[21] J. K. Lee, Y.-G. Kim, Y. S. Chi, W. S. Yun, I. S. Choi, *J. Phys. Chem. B* **2004**, *108*, 7665.
[22] R. M. Nyquist, K. Ataka, J. Heberle, *ChemBioChem* **2004**, *5*, 431.
[23] S. A. Tatulian, B. Chen, J. Li, S. Negash, C. R. Middaugh, D. J. Bigelow, T. C. Squier, *Biochemistry* **2002**, *41*, 741.
[24] P. Rigler, W.-P. Ulrich, P. Hoffmann, M. Mayer, H. Vogel, *ChemPhysChem* **2003**, *4*, 268.
[25] K. Gerwert, G. Souvignier, B. Hess, *Proc. Natl. Acad. Sci. USA* **1990**, *87*, 9774.
[26] K. Gerwert, B. Hess, J. Soppa, D. Oesterhelt, *Proc. Natl. Acad. Sci. USA* **1989**, *86*, 4943.
[27] P. Pelliccioli Anna, J. Wirz, *Photochem. Photobiol. Sci.* **2002**, *1*, 441.

[28] J. A. McCray, D. R. Trentham, *Annu. Rev. Biophys. Biophys. Chem.* **1989**, *18*, 239.
[29] J. E. T. Corrie, D. R. Trentham, *Bioorg. Photochem.* **1993**, *2*, 243.
[30] C.-H. Park, R. S. Givens, *J. Am. Chem. Soc.* **1997**, *119*, 2453.
[31] V. Cepus, C. Ulbrich, C. Allin, A. Troullier, K. Gerwert, *Methods Enzymol.* **1998**, *291*, 223.
[32] R. Masuch, D. A. Moss, *Applied Spectroscopy* **2003**, *57*, 1407.
[33] E. Kauffmann, N. C. Darnton, R. H. Austin, C. Batt, K. *Proc Natl Acad Sci USA* **2001**, *98*, 6646.
[34] R. A. Palmer, J. L. Chao, R. M. Dittmar, V. G. Gregoriou, S. E. Plunkett, *Applied Spectroscopy* **1993**, *47*, 1297.
[35] R. A. Palmer, C. J. Manning, J. L. Chao, I. Noda, A. E. Dowrey, C. Marcott, *Applied Spectroscopy* **1991**, *45*, 12.
[36] O. Weidlich, F. Siebert, *Applied Spectroscopy* **1993**, *47*, 1394.
[37] W. Uhmann, A. Becker, C. Taran, F. Siebert, *Applied Spectroscopy* **1991**, *45*, 390.
[38] R. Rammelsberg, B. Hessling, H. Chorongiewski, K. Gerwert, *Applied Spectroscopy* **1997**, *51*, 558.
[39] B. Hessling, G. Souvignier, K. Gerwert, *Biophys. J.* **1993**, *65*, 1929.
[40] C. Ruckebusch, L. Duponchel, B. Sombret, J. P. Huvenne, J. Saurina, *J. Chem. Inf. Comput. Sci.* **2003**, *43*, 1966.
[41] M. Engelhard, K. Gerwert, B. Hess, F. Siebert, *Biochemistry* **1985**, *24*, 400.
[42] *Biochemistry*, (Ed.: L. Stryer), 4th revised edition, W. H. Freeman, New York, **1996**.
[43] J. Lugtenburg, R. A. Mathies, R. G. Griffin, J. Herzfeld, *Trends Biochem. Sci.* **1988**, *13*, 388.
[44] C. Allin, K. Gerwert, *Biochemistry* **2001**, *40*, 3037.
[45] W. B. Fischer, S. Sonar, T. Marti, H. G. Khorana, K. J. Rothschild, *Biochemistry* **1994**, *33*, 12757.
[46] C. F. W. Becker, C. L. Hunter, R. Seidel, S. B. H. Kent, R. S. Goody, M. Engelhard, *Proc. Natl. Acad. Sci. USA* **2003**, *100*, 5075.
[47] M. Eichinger, P. Tavan, J. Hutter, M. Parrinello, *J. Chem. Phys.* **1999**, *110*, 10452.
[48] M. Klaehn, G. Mathias, C. Kötting, M. Nonella, J. Schlitter, K. Gerwert, P. Tavan, *J. Phys. Chem. A* **2004**, *108*, 6186.
[49] M. Klähn, J. Schlitter, K. Gerwert, unpublished results.
[50] R. Rammelsberg, G. Huhn, M. Lubben, K. Gerwert, *Biochemistry* **1998**, *37*, 5001.
[51] H. Luecke, H. T. Richter, J. K. Lanyi, *Science* **1998**, *280*, 1934.
[52] F. Garczarek, J. Wang, M. A. El-Sayed, K. Gerwert, *Biophys. J.* **2004**, *87*, 2676.
[53] V. Z. Spassov, H. Luecke, K. Gerwert, D. Bashford, *J. Mol. Biol.* **2001**, *312*, 203.
[54] C. Kandt, J. Schlitter, K. Gerwert, *Biophys. J.* **2004**, *87*, 1396.
[55] J. Le Coutre, J. Tittor, D. Oesterhelt, K. Gerwert, *Proc. Natl. Acad. Sci. USA* **1995**, *92*, 4962.
[56] J. Breton, C. Boullais, C. Mioskowski, P. Sebban, L. Baciou, E. Nabedryk, *Biochemistry* **2002**, *41*, 12921.
[57] W. Mäntele in *Biophysical Techniques in Photosynthesis* (Eds.: J. Amesz, A. J. Hoff), Kluwer, Dordrecht, Netherlands, **1996**, pp. 137.
[58] M. Y. Okamura, M. L. Paddock, M. S. Graige, G. Feher, *Biochim. Biophys. Acta* **2000**, *1458*, 148.
[59] M. H. B. Stowell, T. M. McPhillips, D. C. Rees, S. M. Solitis, E. Abresch, G. Feher, *Science* **1997**, *276*, 812.
[60] A. Wittinghofer, *Biol Chem.* **1998**, *379*, 933.
[61] V. Cepus, A. J. Scheidig, R. S. Goody, K. Gerwert, *Biochemistry* **1998**, *37*, 10263.
[62] C. Kötting, K. Gerwert, *Chem. Phys.* **2004**, *307*, 227.
[63] H. R. Bourne, *Nature* **1997**, *389*, 673.
[64] X. Du, G. E. Black, P. Lecchi, F. P. Abramson, S. R. Sprang, *Proc. Natl. Acad. Sci. USA* **2004**, *101*, 8858.
[65] A. Wittinghofer, E. F. Pai, *Trends Biochem. Sci.* **1991**, *16*, 382.
[66] K. Scheffzek, M. R. Ahmadian, W. Kabsch, L. Wiesmuller, A. Lautwein, F. Schmitz, A. Wittinghofer, *Science* **1997**, *277*, 333.
[67] F. Garczarek, L. S. Brown, J. K. Lanyi, K. Gerwert, *Proc. Natl. Acad. Sci. USA* **2005**, *102*, 3633.

Received: October 18, 2004
Published online on April 6, 2005

